ELSEVIER

Contents lists available at ScienceDirect

### Biomedicine & Pharmacotherapy

journal homepage: www.elsevier.com/locate/biopha





### Enhancing non-viral gene delivery to human T cells through tuning nanoparticles physicochemical features, modulation cellular physiology, and refining transfection strategies

Abazar Roustazadeh <sup>a,b</sup>, Maryam Askari <sup>c</sup>, Mohammad Hossein Heidari <sup>c</sup>, Majid Kowsari <sup>a</sup>, Fatemeh Askari <sup>d</sup>, Jalil Mehrzad <sup>e</sup>, Saman Hosseinkhani <sup>f</sup>, Mohsen Alipour <sup>a,b,\*</sup>, Hassan Bardania <sup>g,\*\*</sup>

- <sup>a</sup> Department of Advanced Medical Sciences & Technologies, School of Medicine, Jahrom University of Medical Sciences, Jahrom, Iran
- <sup>b</sup> Department of Biochemistry, School of Medicine, Jahrom University of Medical Sciences, Jahrom, Iran
- <sup>c</sup> School of Medicine, Jahrom University of Medical Sciences, Jahrom, Iran
- d Department of Obstetrics and Gynecology, School of Medicine, Jahrom University of Medical Sciences, Jahrom, Iran
- e Department of Microbiology and Immunology, Faculty of Veterinary Medicine, University of Tehran, Tehran, Iran
- <sup>f</sup> Department of Biochemistry, Faculty of Biological Sciences, Tarbiat Modares University, Tehran, Iran
- g Cellular and Molecular Research Center, Yasuj University of Medical Sciences, Yasuj, Iran

### ARTICLE INFO

# Keywords: Engineered immune cells Gene delivery PEI/DNA nanoparticle Tuning nanoparticles

#### ABSTRACT

Genetically engineered immune cells hold great promise for treating immune-related diseases, but their development is hindered by technical challenges, primarily related to nucleic acid delivery. Polyethylenimine (PEI) is a cost-effective transfection agent, yet it requires significant optimization for effective T cell transfection. In this study, we comprehensively fine-tuned the characteristics of PEI/DNA nanoparticles, culture conditions, cellular physiology, and transfection protocols to enhance gene delivery into T cells. Gel retardation and dynamic light scattering (DLS) analyses confirmed that PEI effectively bound to DNA, forming size- and charge-adjustable particles based on the N/P ratio, which remained stable in RPMI 1640 medium for 3 days at 25°C. At an N/P ratio of 8.0, these nanoparticles achieved an optimal transfection rate, which improved further with adjustments in DNA dosage and complex volume. Additionally, increasing the cell seeding density and adding complete media shortly after transfection significantly boosted PEI-mediated gene delivery. Notably, reversing the transfection in vials resulted in a 20-fold increase in cellular uptake and transfection efficiency compared to the conventional direct transfection method in culture plates. Finally, modifying cellular physiology with hypotonic extracellular media at pH 9.0 dramatically enhanced transfection rates while maintaining minimal cytotoxicity. These findings could reduce the cost and complexity of preparing engineered T cells, potentially accelerating the development of immune cell therapies for human diseases.

### 1. Introduction

Recent efforts to combat immune-related diseases have led to the emergence of immune cell therapies [1–3]. Some of these therapies are FDA-approved for malignancies, with over 500 companies working on their commercialization [4]. Engineered immune cells, such as Chimeric Antigen Receptor (CAR) T-cells, have shown impressive responses in patients unresponsive to other treatments [4–6].

To date, genetic engineering remains the most effective method for

manipulating and empowering immune cells [7,8]. However, the delivery of genetic materials into immune cells is impeded by significant barriers, such as the cell membrane charge, endosome/lysosome degradation, the crowded cytosol, and the nuclear membrane [9,10]. Consequently, numerous research groups are focusing on developing gene delivery methods to overcome these obstacles.

To date, various approaches for gene delivery have been explored, including electroporation, viral vectors, and non-viral carriers. While electroporation allows gene delivery to isolated immune cells, it is

E-mail addresses: m.alipour@jums.ac.ir (M. Alipour), hasan.bardania@yums.ac.ir (H. Bardania).

https://doi.org/10.1016/j.biopha.2025.117820

Received 18 August 2024; Received in revised form 23 December 2024; Accepted 9 January 2025 Available online 20 January 2025

0753-3322/© 2025 The Authors. Published by Elsevier Masson SAS. This is an open access article under the CC BY-NC-ND license (http://creativecommons.org/licenses/by-nc-nd/4.0/).

<sup>\*</sup> Corresponding author at: Department of Advanced Medical Sciences & Technologies, School of Medicine, Jahrom University of Medical Sciences, Jahrom, Iran.

<sup>\*\*</sup> Corresponding author.

restricted to in vitro applications, exhibits high toxicity, and faces challenges related to scalability and cell compatibility [11]. Similarly, viral vectors present issues such as high costs, limited cargo capacity, and risks of immune responses and mutagenesis. These limitations have prompted researchers to seek more reliable non-viral carriers for delivering genes to immune cells [4,12].

Non-viral carriers, including carbonate apatite, iron oxide, liposomes, peptides, gold nanoparticles, and polymers, provide advantages such as ease of production, adaptability, low cost, and better safety compared to viral carriers [3,8,13–15]. Among these, cationic polymers like polyethyleneimine (PEI), poly-L-lysine (PLL), and poly(2-(dimethylamino)ethyl methacrylate) (pDMAEMA) effectively neutralize the anionic charges of nucleic acids, protect them from nucleases, and form nano-sized complexes that facilitate cellular internalization [16].

Among the mentioned polymers, PEI with its star-shaped architecture has garnered significant attention for gene delivery due to its high DNA loading capacity, low cost, scalable synthesis, and proton sponge effect [17]. Its primary, secondary, and tertiary amine groups act as a proton sponge in acidic conditions, reducing lysosomal nuclease activity and promoting endosomal rupture, which facilitates gene delivery [18]. However, the transfection efficiency of PEI/DNA nanoparticles in non-adherent cells, such as T cells, is relatively low. This limitation is likely due to two primary factors: reduced rates of endocytosis and decreased endosome acidification. These challenges diminish the uptake of PEI/DNA nanoparticles through endocytosis and impede their potential for endosomal escape via the proton sponge effect. Consequently, there is an urgent need to develop improved transfection methodologies to overcome these obstacles.

Until now various approaches including, carrier modification, using additive and tuning physicochemical features of nanoparticles have been employed, to enhance the transfection rates achieved by PEI-based polyplexes. For example Uludağ et al. used linoleic substituted PEI to

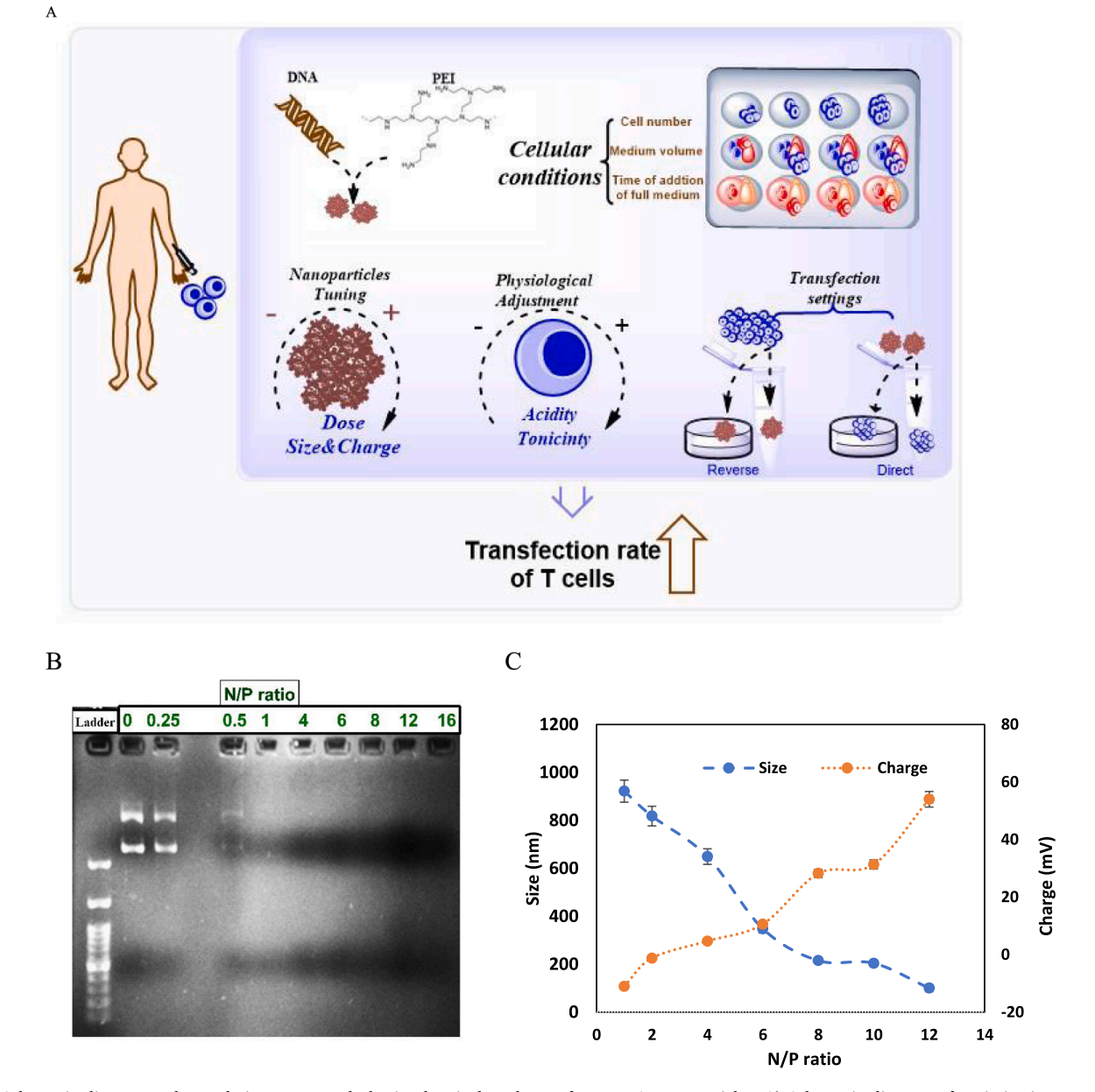


Fig. 1. Schematic diagram, gel retardation assay, and physicochemical analyses of PEI/DNA nanoparticles. A) Schematic diagram of optimization processes for improving gene delivery to T cells. B) Gel retardation assay of PEI/DNA nanoparticles. The nanoparticles were prepared with 0.5  $\mu$ g of pDB2GFP plasmid DNA at different N/P ratios. C) Physicochemical analyses of PEI/DNA nanoparticles. The size and charge of nanoparticles containing 0.5  $\mu$ g of DNA at different N/P ratios were measured using dynamic light scattering.

improve the siRNA delivery into lymphocyte [19]. Avyadevara et al. demonstrated that the addition of Ca<sup>2+</sup> to the culture media significantly improves the efficiency of polyplex-mediated transfection using (PEI), achieving up to a 12-fold increase compared to controls [20]. González-Domínguez et al. optimized the polymer/DNA incubation time to improve gene delivery into mammalians cells [16,21]. More importantly, the PEI/DNA ratio, as well as the size and charge of polyplexes, play critical roles in determining their interactions with cargo, cellular trafficking, and endosomal escape [16,22]. Cheraghi et al. demonstrated that adjusting physicochemical features enhances PEI-mediated gene delivery to breast cancer cells [23]. However, the transfection efficiency achieved by PEI-based polyplexes is cell-dependent, meaning that an optimal formulation for one cell type may not be effective for others [24, 25]. The cell type dependency of polyplex formulations, combined with lower endocytosis rates and reduced endosome acidification in T cells. poses significant challenges in T cell transfection. A comprehensive evaluation of the factors influencing PEI-mediated T cell transfection, which addresses these challenges, is currently lacking. Therefore, there is an urgent need to thoroughly assess various parameters, including nanoparticle optimization, media tonicity, acidity modulation, and transfection modifications, to enhance cellular uptake and gene delivery rates in T cells.

Here, for the first time, we have comprehensively evaluated the impact of tuning the physicochemical properties of PEI-based nanoparticles, optimizing cell culture parameters, modulating cellular physiology, and refining transfection strategies on the transfection rate, aiming to enhance gene delivery efficiency into T cells. For this reason, we complexed PEI with a gene reporter-harboring plasmid to fabricate nano-sized particles. After optimizing the physicochemical properties of the nanoparticles, we transfected Jurkat cells, which serve as a model for T cells (derived from a 14-year-old boy with acute lymphoblastic leukemia), using various approaches to determine the optimal conditions and formulation for gene delivery (Fig. 1a).

### 2. Material and method

### 2.1. Preparation of plasmid DNA

The E. coli bacteria harboring the psiCHEK 2 plasmid were cultured in 10 ml of LB medium containing 10  $\mu g/ml$  of ampicillin for 16 hours. Subsequently, the bacteria were harvested by centrifugation at 4000 RPM for 10 minutes. The bacterial pellets were then used for plasmid extraction using a GeneBox kit, following the manufacturer's protocol. The concentration of the purified plasmid was determined using a NanoDrop Microvolume UV-Vis spectrophotometer (Biotek), and the quality of the plasmid DNA was assessed through agarose gel electrophoresis. For this analysis, the purified plasmid was loaded onto a 1 % agarose gel and run for one hour at 80 V. The gel was subsequently visualized using a UV gel documentation system. Finally, the purified plasmid was aliquoted and stored at  $-20\ ^{\circ}\text{C}$  for future experiments.

### 2.2. Preparation of nanoparticles

The branched 25 kDa polyethyleneimine (PEI) (Sigma) was diluted to a concentration of 1 mg/ml in deionized water for subsequent investigations. The nanoparticles were synthesized by mixing branched 25 kDa PEI and psiCHEK 2 DNA for 30 minutes at room temperature. The mixing ratio of polymer and DNA was based on molar ratio of amine groups in PEI and phosphate groups in DNA according to following formula:

N P ratio : 
$$\frac{Weight of PEL[(yg)]}{Molecular weight of repeated unit Number of positive charge  $\frac{Number of positive charge}{Weight of DNA(\mu g)}$$$

Each repeat unit of polyethylenimine (PEI) with a molecular weight of 25 kDa has an approximate molecular weight of 473 daltons (Da), and the number of positive charges per repeat unit is typically around four. In a DNA strand, the average molecular weight per nucleotide is approximately 330 Da. For example, nanoparticles at the N/P ratio of 1 were prepared by addition of 0.35  $\mu$ l of PEI (1 mg/ml) to a vial containing 1  $\mu$ g of plasmid DNA. Following the addition of PEI, the mixture was gently pipetted 30 times and allowed to undergo complexation at 25°C for 30 minutes.

### 2.3. Gel retardation assay

The DNA binding capacity of PEI-based nanoparticles was evaluated using a gel retardation assay. For this purpose, nanoparticles were prepared with  $0.5\,\mu g$  of DNA at various N/P ratios. The prepared nanoparticles, which contained 1X loading dye, were loaded into a 1 % agarose gel in 1X TAE buffer and electrophoresed for 45 minutes at 80 V. The gel was stained with SafeStain and visualized using UV illumination with a gel documentation system (Syngene).

### 2.4. Nanoparticles size, charge and morphology studies

The size and surface charge of DNA/PEI polyplexes were evaluated using dynamic light scattering analysis. Briefly, nanoparticles were prepared by 0.5  $\mu g$  of plasmid DNA at various N/P ratios. The volumes of the mixtures were adjusted to 500  $\mu l$  with deionized water and analyzed using a Nano-Zeta Sizer (Nanotrac Wave II). Experiments were conducted in triplicate. For Transmission electron microscopy (TEM) analysis, the nanoparticles were prepared by 1  $\mu g$  of plasmid DNA at N/P ratios of 2 and 8. After 25 minutes, the nanoparticles were drop-cast onto carbon-supported copper grids. The grids were then stained with 2 % uranyl acetate for 2 minutes, and any excess liquid was absorbed using filter paper. The grids were air-dried and examined using a transmission electron microscope (TEM, Zeiss - EM100 kV).

### 2.5. Serum stability analysis

One of the main problems in gene delivery is the susceptibility of DNA to nuclease degradation. To assess the DNA protection capability of PEI, nanoparticles were prepared at an N/P ratio of 8, and 10 % serum was added to them. These complexes were incubated for 1 hour at 30°C, after which sodium salt of heparin at a concentration of 1 mg/ml was added to facilitate the release of DNA from the complexes. The samples were then loaded onto a 1 % agarose gel and subjected to electrophoresis for 45 minutes at 80 V. The gel was visualized using UV illumination with a gel documentation system.

### 2.6. Cell culture and transfections

The Jurkat cells were obtained from the Pasteur Institute and maintained in a 5 % humidified CO2 incubator. The cells were cultured in a T25 flask using RPMI 1640 medium supplemented with 10 % fetal bovine serum (FBS) and 1 % penicillin-streptomycin. Cell viability was assessed using trypan blue dye exclusion method. Transfection was carried out as described below, unless otherwise specified for modified experiments. On the day of transfection,  $5 \times 10^5$  cells were cultured in a 24-well plate in 100 μl of serum-free RPMI 1640 medium. Nanoparticles composed of PEI/DNA containing 0.5 µg of psiCHEK-2 plasmid were prepared at various N/P ratios. The prepared nanoparticles were diluted to a final volume of  $100\,\mu l$  with serum-free RPMI1640 medium and added dropwise to the plate. In the case of reverse transfection, the prepared polyplexes were added to the plate, and the volume was adjusted to 100 µl with serum-free RPMI medium, followed by the addition of a suspension of  $5 * 10^5$  cells to the nanoparticles. Full media were added to the cells two hours later.

The transfection protocol was modified in several aspects, including

the amount of DNA in nanoparticles (0.25-4 µg), the volume of media for complex dilution (25-150 µl), the presence of serum in the transfection medium (with and without FBS), the volume of media for cell suspension (25-100 µl), and the time span of incubation before the addition of complete media (spanning from 5 minutes to 2 hours). For transfection at various pH values, one hour after the addition of a  $50 \, \mu l$ complex to the cells, RPMI media prepared at different pH values were added to the cells. The effect of tonicity on the transfection efficiency of PEI/DNA complexes was also evaluated by adjusting the tonicity of the cell culture media using sterile NaCl solution. This adjustment was made both prior to and after the addition of the complexes. After 48 hours of incubation in a cell culture incubator, the cells were harvested by centrifugation at 4000 RPM for 10 minutes and subsequently lysed with CCLR buffer. A total of 10 µl of cell lysate was mixed with 10 µl of luciferase substrate, and luciferase activity was evaluated using a BMG luminometer.

### 2.7. Transfection in vial

For transfection in vial,  $2\times10^\circ5$  Jurkat cells were suspended in serum-free RPMI medium in a 1.5 ml microtube (Eppendorf tubes). The vial cap was punctured under sterile conditions to facilitate the exchange of CO2 and O2. The nanoparticles of PEI/DNA were prepared using 0.5 µg of DNA at various N/P ratios and diluted to a final volume of 100 µl with RPMI medium, prior to addition to the cells. For reverse transfection, an alternative method of nucleic acid delivery, a suspension of  $2\times10^\circ5$  Jurkat cells was added to the polyplexes suspension prepared in a 1.5 ml micro tube on the day of transfection. Two hours later, 200 µl of RPMI medium supplemented with fetal bovine serum and penicillin-streptomycin was added to the vial. After 48 hours, the vial was centrifuged at 4000 RPM for 5 minutes, and the supernatant was discarded. The pellet was then lysed with CCLR buffer and luciferase activity was measured as previously described.

### 2.8. Cytotoxicity assay

The effects of free PEI and PEI complexed with DNA were evaluated using MTT assay. For this purpose, the  $1\,^{*}\,10^{4}$  Jurkat cells were cultured in a 96-well plate and maintained in a humidified  $CO_2$  incubator. The cells were treated with free PEI and/or PEI/DNA nanoparticles at various N/P ratios prepared using 0.5  $\mu g$  of DNA, or with nanoparticles prepared with different DNA concentrations at various N/P ratios for 48 hours. Subsequently, 10  $\mu l$  of a 5 mg/ml MTT solution was added to the cells and incubated for 4 hours. Then 100  $\mu l$  of DMSO was added to the solution and incubated at 37 °C for 30 minutes. The absorbance of cells at 570 nm was measured using a UV–visible plate reader. Nontransfected cells were used as a control to normalize obtained raw absorbance. The experiment was performed in triplicate.

### 2.9. DNA binding and release analyses

To determine the DNA binding rate to PEI, nanoparticles with N/P ratios of 2.0 and 8.0 were diluted with deionized water to achieve a final volume of 30  $\mu l$ . The mixture was incubated for varying durations, ranging from 1 to 30 minutes, and then centrifuged at 17,000 g for 3 minutes. After centrifugation, the concentration of unbound DNA in the supernatant was analyzed using a UV-Vis NanoDrop spectrophotometer. The amount of bound DNA at each time point was calculated by subtracting the concentration of unbound DNA from the total amount of DNA initially used. For the release study, nanoparticles with N/P ratio of 2.0 and 8.0 were diluted with deionized water to a final volume of 100  $\mu l$  and incubated in a shaker incubator at 25°C for one week. At predetermined time intervals, the nanoparticles were centrifuged at 17,000 g for 10 minutes. A volume of 20  $\mu l$  of the supernatant was replaced with an equal volume of deionized water. The amount of DNA in the supernatant was analyzed using a UV-Vis NanoDrop

spectrophotometer (Biotek). The percentage of DNA mass released was calculated by dividing the mass released at a specific time point by the total initial mass of DNA. Additionally, the cumulative percentage of DNA mass released at each time point was determined by dividing the cumulative mass released by the total initial mass of DNA.

### 2.10. Evaluation of cellular uptake of PEI/DNA nanoparticles

To analyze the effects of various conditions on the cellular uptake of PEI/DNA, nanoparticles containing 1 µg of FAM-labeled DNA were used for transfection. Jurkat cells were cultured in RPMI 1640 medium in a humidified CO<sub>2</sub> incubator. On the day of transfection,  $2 \times 10^5$  cells were seeded in a 24-well plate, and RPMI 1640 medium supplemented with a PEI/DNA complex at an N/P ratio of 8 was added as a control. In another experimental condition, the tonicity of the medium was changed to hypotonic by adding an equal volume of deionized water, before and after the addition of the complex. Additionally, to assess the effect of pH on transfection, the cell culture media were adjusted to pH values of 5.0 and 9.0, respectively, 30 minutes after the addition of the complex. For reverse transfection, after preparing the complexes, their volumes were adjusted to 100 µl using either RPMI 1640 or the same medium supplemented with an equal volume of deionized water. Then,  $2 \times 10^5$ Jurkat cells, also prepared in either RPMI 1640 or the same medium supplemented with an equal volume of deionized water, were added to the complexes in a dropwise manner. After 3 hours, the cells were washed with phosphate-buffered saline (PBS) containing 0.04 % Trypan Blue to quench extracellular fluorescence. The cells were then analyzed using a Nikon Eclipse Ts2 Inverted Microscope. The number of fluorescent cells was counted using NIS-Elements Basic Research software (Nikon).

### 2.11. Evaluating the storage stability of PEI/DNA nanoparticles

To evaluate the stability of the particles during storage, PEI/DNA nanoparticles were prepared at an N/P ratio of 8 using 1  $\mu$ g of plasmid DNA. The nanoparticles were then diluted in various buffers, including deionized water, phosphate-buffered saline (PBS), and RPMI 1640. After 25 minutes, the nanoparticles were stored under various temperature conditions, including -20 °C, 4 °C, and 25 °C. At specified time intervals (1, 3, 5, and 7 days), the nanoparticles were analyzed using gel electrophoresis and dynamic light scattering (DLS).

### 3. Results and discussion

### 3.1. The DNA binding capacity of nanoparticles

The first step in the preparation of nanoparticles is the binding of DNA to carrier. The DNA binding capacity of the nanocarrier at different N/P ratios was evaluated by gel retardation assay. As shown in Fig. 1b, the PEI at N/p ratio of 0.25-0.5 began to decrease electrophoretic movement of pDNA compared to control DNA. In other words, at the mentioned N/P ratios PEI binds to DNA partially. However, the increase of carrier content, impeded the electrophoretic movement of DNA, so that at an N/P ratio of 1, the PEI completely retarded the electrophoretic movement of DNA and showed a shiny band in the well. These results are consistent, with our previous report, which indicated that at N/P ratio of 1, the cationic carrier completely bound to pDNA and stopped its electrophoretic mobility[26]. Additionally, with increase of N/P ratio a lower emission was observed in the wells. This result suggests the formation of tight particles that exclude the dye from DNA at high N/P ratio. Therefore, complexation of PEI and DNA with an N/p ratio of higher than 0.5 is essential for the fabrication of suitable, compact nanoparticles. The formation of condensed nanoparticles has been reported that can protect DNA from serum and intracellular nucleases, as well as to enhance the transfection rate [27].

### 3.2. Nanoparticles size, charge and morphology

The size and charge of particles, as two key features, ascertain the interactions between particles, stability in cell culture media, and interactions with cell membranes and cytosolic components. Therefore, in this study, prior to proceeding with transfection study, we evaluated the size and charge of nanoparticles at various N/P ratios using Dynamic Light Scattering analysis. The nanoparticles at an N/P ratio of 1 exhibited a hydrodynamic diameter of approximately 900 nm. As shown in Fig. 1c the increase of carrier content decreased nanoparticle size, so that at an N/P ratio of 8, we observed particles with a size of around 200 nm. This result, consistent with the gel retardation assay, demonstrated that, the increase in carrier content led to the formation of more compact particles. It has been reported that this formation of compact particles occurs through a self-assembly process[21]. Moreover, the small size of the particles is suitable for uptake via the endocytosis

process [28]. Surface charge, another key characteristic of polyplexes, is known as an important factor influencing nonspecific interactions with the plasma cell membrane and, consequently, the uptake route of nanoparticles. Therefore, we also evaluated the surface charge of nanoparticles as a function of the N/P ratio. Naked DNA exhibited a negative zeta potential, which is consistent with the negatively charged phosphate groups in the DNA backbone. Furthermore, the PEI/DNA complex at an N/P ratio of 2 demonstrated a zeta potential of + 1 mV, suggesting that PEI binds to DNA and neutralizes its negative charge. As the N/P ratio increased, we observed a corresponding rise in the zeta potential of the nanoparticles. This positive charge on the nanoparticles facilitates their interaction with the negatively charged components of the cell membrane, thereby initiating cellular uptake processes [29]. To validate the formation of nanoparticles and evaluate the effect of the N/P ratio on their morphology, we conducted transmission electron microscopy (TEM) analysis. Based on DLS results, nanoparticles with

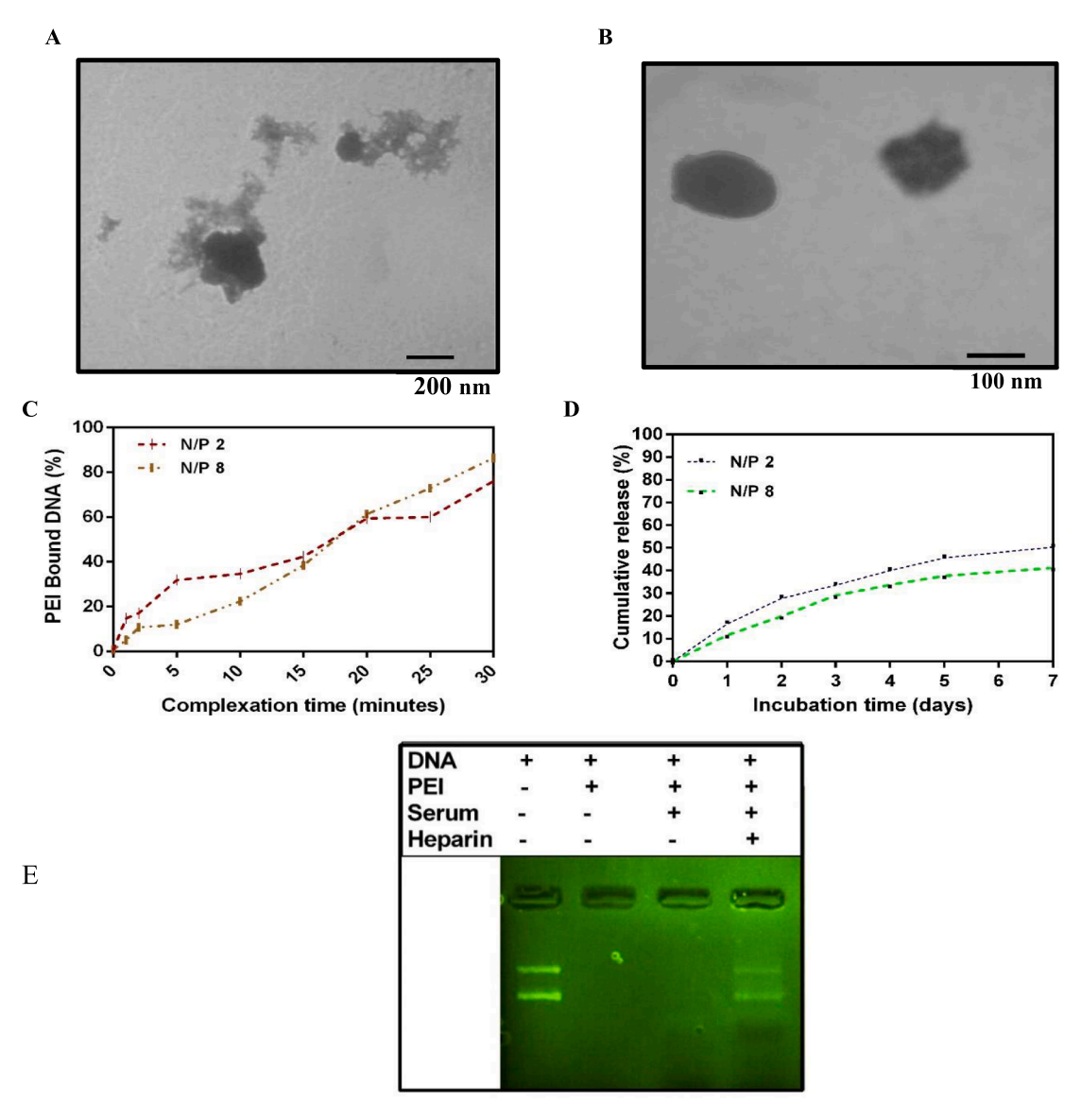


Fig. 2. Evaluation of the morphology, DNA binding rate to PEI, DNA release rate, and serum stability of nanoparticles. A) Transmission electron microscopy (TEM) image of PEI/DNA nanoparticles at an N/P ratio of 2. B) TEM image of PEI/DNA nanoparticles at an N/P ratio of 8. C) The kinetics of DNA binding to PEI at different N/P ratios were studied. The prepared DNA was incubated with PEI for various time points. After incubation, the unbound DNA was separated by centrifugation, and its concentration was measured. This concentration was then used to calculate the amount of PEI-bound DNA. D) The kinetics of DNA release from PEI/DNA nanoparticles at different N/P ratios were studied. The amount of released DNA was measured using a UV-Vis spectrophotometer. E) Serum stability analysis of PEI/DNA nanoparticles. DNA protection potential of PEI nanocarriers against serum nucleases was studied. PEI/DNA nanoparticles were prepared using 1 μg of DNA, and heparin was used to release the DNA from nanoparticles incubated in the presence of serum.

N/P ratios of 2 and 8 were selected for TEM analysis due to their significant size differences, which allowed for a detailed structural investigation. As illustrated in Fig. 2a and b, the complexation of DNA with PEI led to the formation of particles with different sizes and morphologies depending on the N/P ratio. At an N/P ratio of 2, TEM revealed irregularly shaped particles with a less compact size of approximately 700 nm. In contrast, increasing the N/P ratio to 8 resulted in more spherical and uniform particles with a size around 160 nm, consistent with the DLS results. This variation in particle size and morphology as a function of the N/P ratio suggests that increasing the PEI content enhances intra-particle ionic interactions, leading to the formation of more condensed particles with well-defined structures. These structural changes not only affect particle stability but also influence the effectiveness of these nanoparticles in interacting with cell membranes and releasing their DNA cargo for gene expression. It is important to note that the observed discrepancies in nanoparticle size between DLS and TEM analyses arise from their differing measurement principles. DLS measures the hydrodynamic radius in solution, incorporating contributions from hydration shells—especially for particles with complex geometries—, while TEM provides direct imaging in a dried state [30].

### 3.3. Binding and release rates of PEI/DNA complexes

One of the primary factors influencing gene delivery systems is their capability to bind DNA at a suitable rate. For this purpose, we analyzed the binding kinetics between DNA and PEI at N/P ratios of 2 and 8. As shown in Fig. 2c, after 1 minute, the amount of unbound DNA at both N/ P ratios remained high, resulting in a binding percentage of slightly below 5 % for nanoparticles at an N/P ratio of 8 and 16 % for those at an N/P ratio of 2, indicating negligible initial binding. This suggests that PEI molecules require time to effectively interact with DNA molecules. However, DNA binding progressively increased with incubation time, so that at 10 minutes, the percentage of bound DNA was approximately 22 % at an N/P ratio of 8 and 40 % at an N/P ratio of 2, respectively. The time-dependent binding indicates that the process is driven by the gradual formation of electrostatic interactions between the positively charged PEI and negatively charged DNA. A significant increase in binding efficiency was observed between 10 and 20 minutes, highlighting a strong interaction facilitated by electrostatic attraction. After 20 minutes, nanoparticles at an N/P ratio of 8 exhibited a higher binding percentage than those at an N/P ratio of 2, suggesting that a higher concentration of PEI enhances binding efficiency due to increased availability of positively charged sites for interaction with DNA. The binding percentage continued to rise steadily, reaching approximately 80 % at 30 minutes, indicating that most available DNA had bound to PEI. This observation aligns with our findings of the transition from loose to compact particles from 5 to 25 minutes. The high binding efficiency and stable complex formation make PEI an effective vector for DNA delivery. In a separate investigation, we analyzed the DNA release rate from the PEI carrier at N/P ratios of 2 and 8, utilizing centrifugation to separate bound and unbound DNA. As shown in Fig. 2d, the nanoparticles with an N/P ratio of 2 rapidly released approximately 20 % of their DNA content within 24 hours. The cumulative release increased with prolonged incubation times, reaching 30 % after 2 days. In contrast, nanoparticles with an N/P ratio of 8 released only 20 % of their DNA content after 2 days. This finding is consistent with dynamic light scattering (DLS) results, which indicated a compact size of approximately 200 nm for nanoparticles at an N/P ratio of 8, while those at an N/P ratio of 2 exhibited a loose structure with a diameter of around 800 nm. After 5 days, the remaining DNA in nanoparticles at both N/P ratios was released at a slower rate. This outcome aligns with the findings reported by Amani et al., which indicated that DNA was released from PEI after 5 days [31].

### 3.4. Evaluation of serum stability of PEI/DNA nanoparticles

The presence of serum and intracellular nucleases poses significant challenges for gene delivery systems. In this study, we investigate the capability of the PEI carrier to protect DNA from degradation by nucleases. As shown in Fig. 2e, similar to the results of the gel retardation assay, the complex remains stable in serum and does not release its DNA component. Subsequently, heparin induced the release of DNA from the PEI complexes. The released DNA exhibited a similar electrophoretic pattern to that of control plasmid DNA, indicating that the PEI carrier effectively protects its DNA cargo from degradation. The results demonstrated that serum components do not disassemble the PEI/DNA complexes. This finding paves the way for transfection in the presence of serum, facilitating future in vivo delivery. Furthermore, investigating the susceptibility to nucleases in the presence of various serum components offers a more realistic environment for analysis. Overall, the results indicate that the nanoparticles can effectively protect DNA from nucleases. A similar finding was reported by Cheraghi et al., which demonstrated that a peptide-based carrier also protected DNA from serum nucleases [27]. It should be noted that while SDS easily induces the release of DNA from peptide carriers, it is not as effective for PEI.

### 3.5. The impact of N/P ratios on the transfection efficiency of nanoparticles

Low cellular internalization and endosomal entrapment are known as the primary barriers to nanoparticle-mediated transfection, undermining the efficiency of non-viral gene delivery to T cells [4,32]. One of the key features of polymeric nanoparticles implicated in overcoming these barriers is their N/P ratios. Therefore, we examined the transfection efficiency of nanoparticles prepared with GFP and/or luciferase genes harboring plasmids at various N/P ratios. As shown in Fig. 3a, the number of GFP-positive cells varied with N/P ratio and time post-transfection. The number of GFP-positive cells increased with an increase in the N/P ratio of nanoparticles up to 8. However, at higher N/P ratios the number of GFP-positive cells remained constant at 16 hours post-transfection. At 48 hours, the highest number of GFP-positive cells was observed at an N/P ratio of 2.00, followed by a decrease at 4.00, a plateau at 6.00, and a slight increase at 8.00. The observed decrease in GFP-positive cells at certain N/P ratios and time points could be attributed to the potential cytotoxic effects of GFP. Studies have shown that GFP can induce cytotoxicity in cells, leading to cell death and a subsequent decrease in the number of GFP-positive cells over time [33]. To obtain a quantitative justification, we prepared nanoparticles containing a luciferase gene-harboring plasmid at various N/P ratios. As shown in Fig. 3b, the highest luciferase activity was observed in Jurkat cells transfected with nanoparticles at an N/P ratio of 8, indicating that this is the optimal ratio for transfection. According to DLS results, nanoparticles at this N/P ratio exhibited a size around than 200 nm, which is consistent with the suitable size of particle for endocytosis. The lower luciferase activity in the lysate of cells transfected with nanoparticles at N/P ratios lower than of 8 may be attributed to the lower polymer content, which in turn leads to a lower concentration of unprotonated amino moieties, which decreases the capacity of the nanoparticles to induce endosomal escape via the proton sponge effect. [18]. Similarly, Pol-L-lysine-based nanoparticles, due to their inability to escape from endosomes, did not demonstrate any transfection capacity in cells[34]. Furthermore, the decrease in transfection efficiency of nanoparticles at very high N/P ratios is presumably attributed to their increased compactness, which results in a slower release of DNA compared to lower N/P ratios. Overall, unlike PLL-based nanoparticles, which necessitate an additional agent like a targeting ligand for effective gene delivery to T cells, PEI-based nanoparticles can independently facilitate gene delivery to these cells [20]. Therefore, as our results indicate, similar to the findings reported by another group, modulating the N/P ratio of PEI-based nanoparticles enhances their transfection

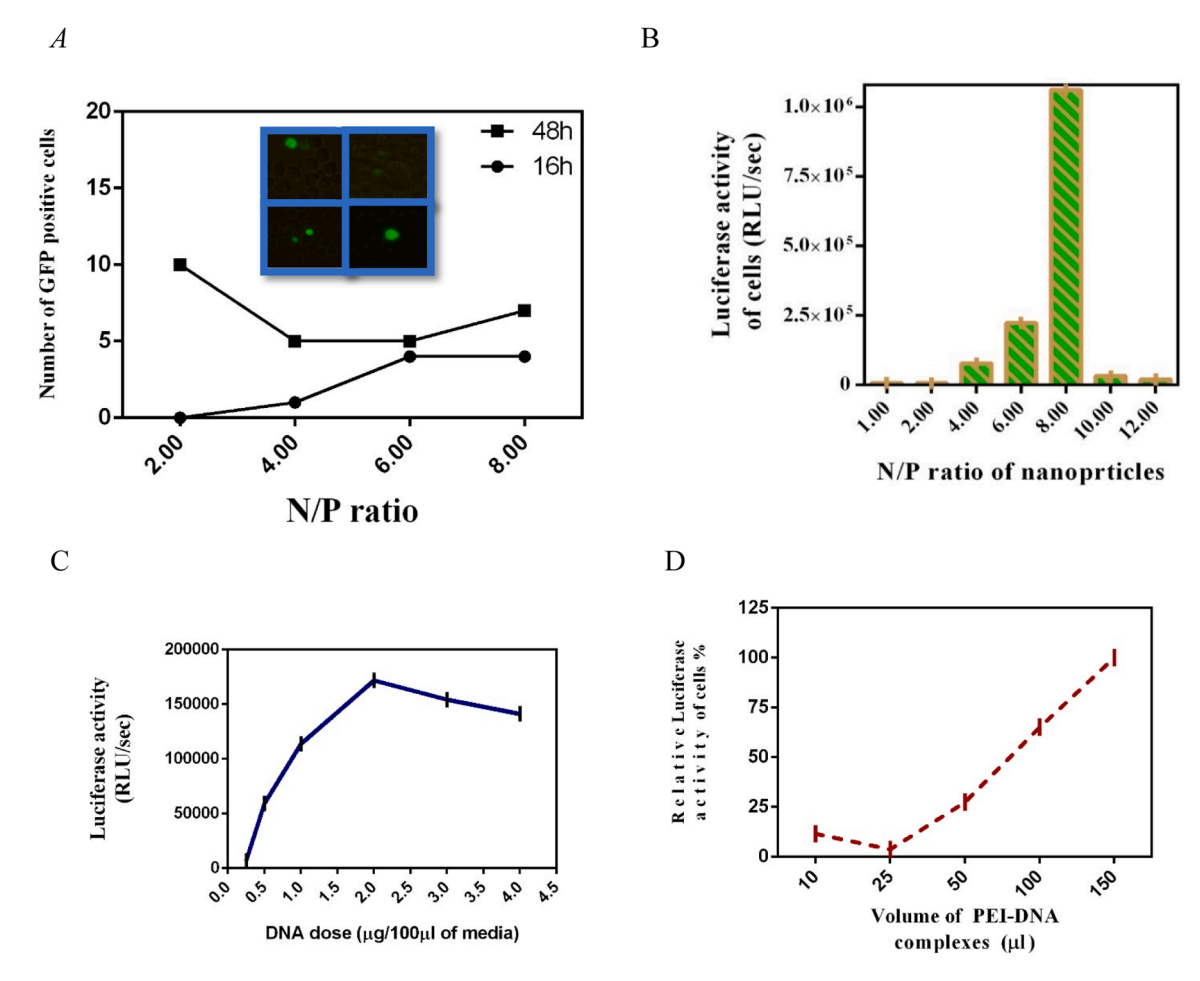


Fig. 3. The effect of modulation of nanoparticles' physicochemical features on T cells transfection. A) The impact of the N/P ratios of nanoparticles prepared with GFP gene harboring plasmid on the transfection of Jurkat cells. Transfection with 0.5  $\mu$ g of GFP plasmid was assessed at 16 and 48 hours post-transfection. The inset images display various GFP-positive cells. B) The quantitative effect of the N/P ratios of PEI/DNA nanoparticles on gene delivery to T cells. Jurkat cells were transfected with 0.5  $\mu$ g of psichek2 plasmid at different N/P ratios. C) The effect of DNA quantity on transfection efficiency. Jurkat cells were transfected with nanoparticles prepared with different amounts of DNA in a 24-well plate. D) The effect of complex volume on the transfection efficiency of PEI/DNA nanoparticles. Complexes of PEI/DNA were diluted with different volumes of medium and used to transfect Jurkat cells.

efficiency [1].

## 3.6. Evaluation of the effect of DNA dosage of nanoparticles on transfection efficiency

One of the most effective strategies for enhancing protein expression is increment of the dosage of DNA, which serves as the main template for mRNA production. Therefore, we sought to determine the appropriate DNA dosage and, correspondingly, the suitable dosage of nanoparticles for the transfection of Jurkat cells. As shown in Fig. 3c, an increase in the quantity of nanoparticles, while maintaining a constant N/P ratio, resulted in enhanced luciferase protein expression. The peak luciferase activity was observed in the lysate of Jurkat cells transfected with nanoparticles containing 2 µg of DNA. In contrast, increasing the DNA concentration beyond 2 µg during the preparation of nanoparticles at a constant N/P ratio led to a decline in luciferase activity, which can be attributed to nanoparticle-associated cytotoxicity at elevated concentrations. A similar outcome was observed with other polycationic polymers in Jurkat cells[29]. Therefore, we selected 1 µg of DNA as the optimal dosage for the preparation of nanoparticles and gene delivery studies.

# 3.7. Evaluation of the effect of volume of complex of PEI/DNA nanoparticles on transfection efficiency

The volume of complexation of DNA-polymer nanoparticles is a critical parameter affecting both intra- and inter-particle interactions, as well as their interactions with target cells. In this study, we evaluated the impact of this volume on the efficiency of nanoparticle-mediated transfection in Jurkat cells. As shown in Fig. 3d, cells transfected with nanoparticles prepared and suspended in a high volume of medium exhibited significantly higher luciferase activity compared to those transfected with nanoparticles prepared and suspended in a low volume. The high transfection efficiency observed with highly diluted nanoparticles can be attributed to two main factors. First, it likely prevents nanoparticle aggregation by reducing particle interactions and decreasing serum content in the final transfection media. Second, the volume of complexation affects DNA compression kinetics and nanoparticle structures, ultimately influencing the transfection rate. Notably, other research groups have also observed increased transfection rates when complexes are formed in higher volume media [29].

### 3.8. The effect of cell seeding density

The cell density is a critical factor influencing nutrient levels for cell growth, as well as the accumulation of cellular debris and excretory metabolites. More importantly, the seeding density of cells ascertains

the number of target sites available for nanoparticles. Therefore, we examined the transfection efficiency of nanoparticles at various cell seeding densities. As shown in Fig. 4a, increasing the seeding density from 500 cells/µl resulted in enhanced luciferase gene activity and the highest transfection efficiency observed at 2000 cells/µl. Consequently, this cell density was selected for further experiments. Specifically, 20and 40-fold increase in transfection efficiency was observed with 2- and 4-fold increase in the number of seeded cells, respectively. This significant increase in transfection efficiency with rising cell numbers per volume of medium is presumably due to the increased local concentration of IL-2, which in turn increases the proliferation rate [35,36]. Indeed, the transient disruption of the nuclear membrane during proliferation improves the efficiency of nuclear gene delivery [37]. In other words, this result may be attributed to a higher number of cells being in the mitotic phase, during which the nuclear membrane is compromised. allowing PEI/DNA nanoparticles to enter the nucleus more easily. Similarly, another study reported that increasing the number of cells per well significantly improved transfection rates [38]. This finding further indicates that transfection efficiency is dependent on cell number. However, as the cell number increased to 4000 cells/µl, the transfection efficiency abruptly declined, presumably due to a decrease in capacity and nutrients for cell growth.

### 3.9. Evaluation of the effect of volume of cell suspension on transfection efficiency

In the next step, considering the importance of media volume on

molecular spacing and the interaction of nanoparticles with cells for membrane crossing, we evaluated the effect of the volume of media in which cells are suspended on transfection efficiency. As shown in Fig. 4b, an increase in the media volume of the cell suspension resulted in enhanced gene delivery and the maximum luciferase activity was observed with a cell suspension prepared at 100  $\mu l$  prior to transfection in a 24-well plate. Beyond this volume, we observed a decrease in the transfection rate. This finding suggests that optimal interaction between nanoparticles and cells occurs at 100  $\mu l$ , leading to enhanced uptake and, consequently, optimal transfection efficiency.

### 3.10. Evaluation of the effect of the timing of the addition of complete medium

In the next step, we evaluated the effect of serum presence in the transfection medium. As shown in Fig. 4c, the presence of FBS in the cell suspension prior to the addition of nanoparticles decreased luciferase activity by around 40 %. This data suggests that serum in the medium negatively impacts the transfection efficiency of Jurkat cells with PEI/DNA complexes, likely due to serum proteins interacting with the complexes, leading to aggregation or instability, which hinders cellular uptake and gene expression. An experiment conducted by another group indicated that the transfection rate of HEK 293 cells was significantly reduced in the presence of medium supplemented with FBS [39]. Therefore, full media containing FBS is typically added to the transfected cells after a lag time. To determine the optimal timing for the addition of FBS-containing medium to transfected cells, we measured

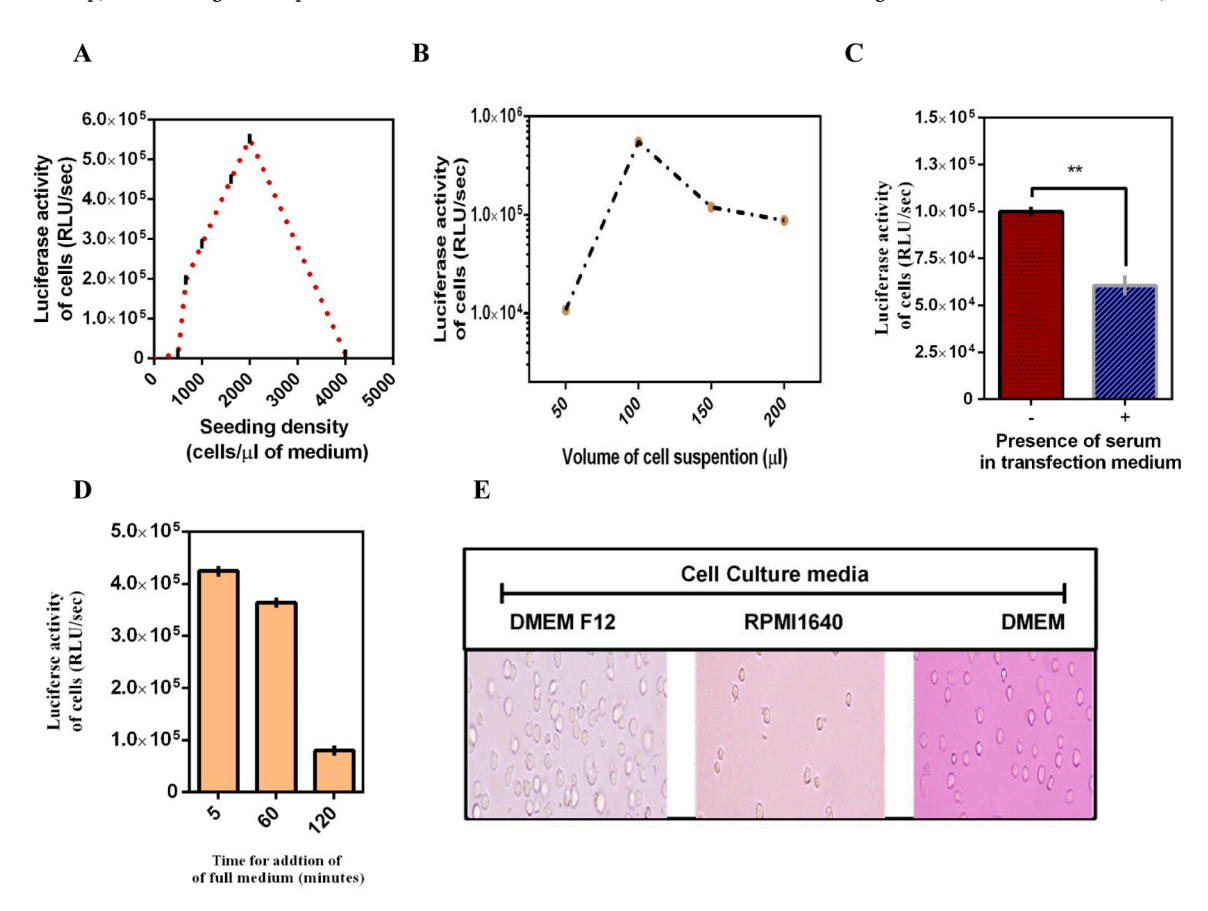


Fig. 4. Evaluation of cell culture conditions on transfection of T cells by PEI/DNA nanoparticles. A) The effect of cell seeding density on transfection efficiency. Jurkat cells at various densities were transfected with PEI/DNA nanoparticles. B) The effect of the volume of cell suspension medium on the transfection efficiency of T cells. The medium was added to the cells prior to the addition of the nanoparticles. C) Assessment of the effect of serum on the transfection potential of PEI/DNA nanoparticles. Jurkat cells were transfected using PEI/DNA at an N/P ratio of 8.0, both in the presence and absence of FBS in the transfection medium. D) The effect of the timing of full medium addition on transfection efficiency. After the addition of PEI/DNA to Jurkat cells, the full medium was added at different time points. E) Morphology of Jurkat cells in different transfection media.

the luciferase activity of Jurkat cells that received the complete medium at various lag time points. As shown in Fig. 4d the maximum luciferase activity was observed in transfected cells that received full media after 5 minutes. When this time was extended to 2 hours, we observed an 8-fold decrease in transfection efficiency. The higher transfection rate observed when complete medium is added shortly after transfection is presumably due to the fact that the addition of FBS at shorter intervals reduces the unwanted toxicity associated with nanoparticles. Furthermore, addition of serum-containing medium with a shorter lag time may decrease nanoparticle aggregation and promote cellular adhesion of nanoparticles. A similar result was reported by another research group [22]. This finding aligns well with results from a different study, which suggested that a brief exposure of approximately 10 minutes is sufficient for nanoparticles to bind to the cell membrane[20]. In contrast, a prolonged lag time for the addition of full medium may increase nanoparticle-mediated toxicity and particle aggregation, ultimately resulting in lower transfection efficiency [39]. Moreover, we evaluated the growth and morphology of Jurkat cells in different cell culture media. Microscopic images demonstrated that, in DMEM and RPMI 1640, these cells exhibited a healthy morphology (Fig. 4e).

### 3.11. Transfection settings: in vial and plate

One of the main steps in transfection is cell culture in various containers, including plates and vials. The three-dimensional shape of the container used for cell suspension significantly influences the rate of contact between cells and nanoparticles. To evaluate the effect of the three-dimensional shape of these containers on PEI-mediated transfection of Jurkat cells, we compared transfection efficiency in vials and plates. As shown in Fig. 5a, the transfection of Jurkat cells with PEI/DNA nanoparticles in vials resulted in a 20-fold increase in luciferase activity compared to the transfection of Jurkat cells in plates under identical conditions. This observation demonstrates that the shape and volume of the cell culture containers can modulate the interactions between cells and nanoparticles; specifically, the narrow space at the bottom of the vial enhances these interactions. Additionally, positioning the transfection tube upright increases the local concentration of cells and nanoparticles. More importantly, gravity provides a physical force that enhances the rate of interaction between cells and nanoparticles in the vial, thereby improving transfection kinetics. Similarly, some research groups have employed centrifugation and/or external magnetic fields to

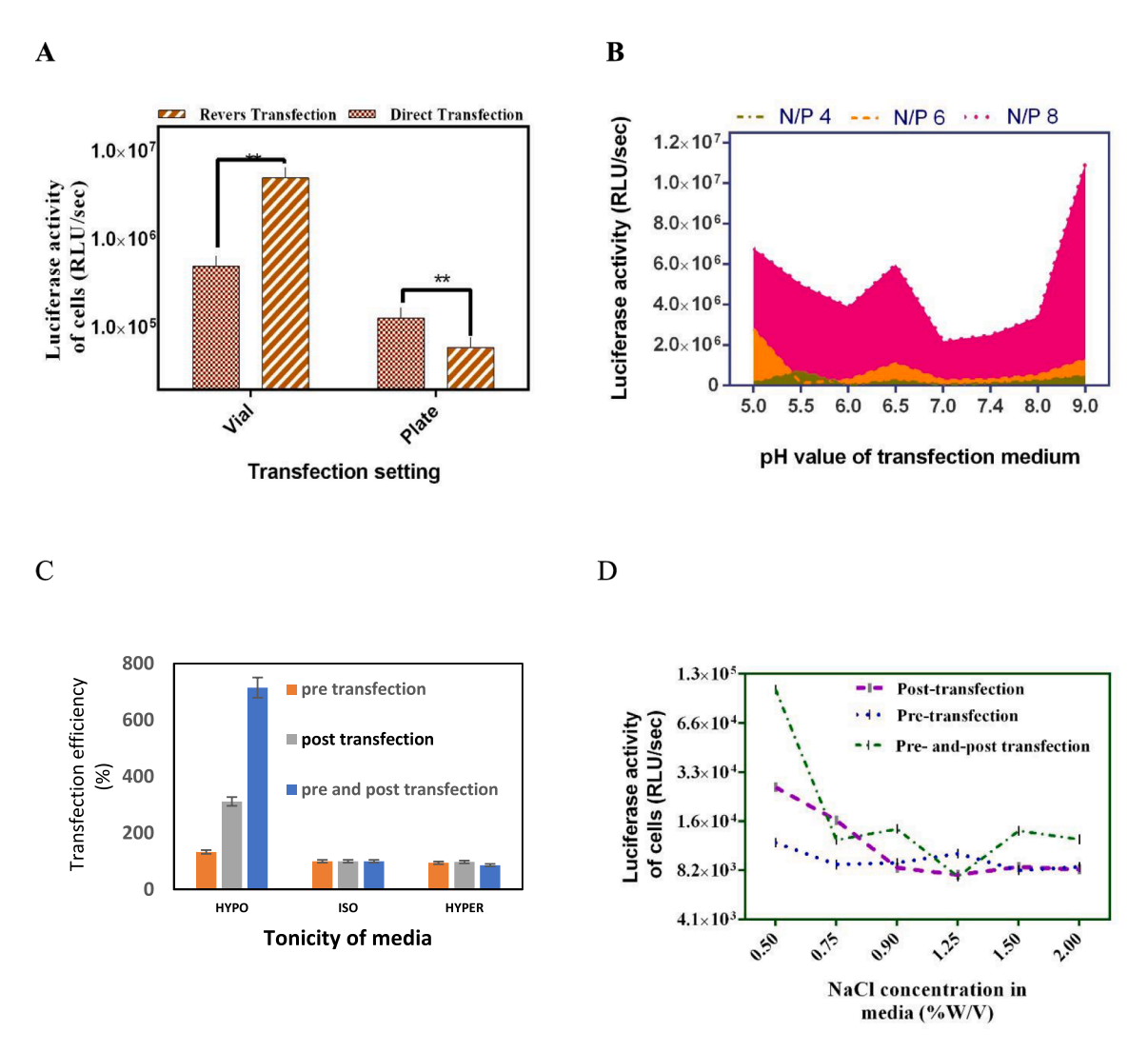


Fig. 5. The effect of transfection settings and modulation of cellular physiology on transfection efficiency. A) The effect of transfection settings on the efficiency of PEI-mediated gene delivery to T cells. Jurkat cells were transfected in vials and/or plates, utilizing either direct addition of nanoparticles to cultured cells or reverse addition of cell suspensions to nanoparticles. B) The effect of transfection medium acidity on the efficiency of PEI-mediated gene delivery to T cells. Jurkat cells were transfected in media prepared with various acidity levels, using PEI/DNA nanoparticles at different N/P ratios. C & D) The effect of transfection medium tonicity on the efficiency of PEI-mediated gene delivery to T cells. Jurkat cells were transfected with PEI/DNA nanoparticles in media with different tonicities (HYPO: hypotonic, ISO: isotonic, and HYPER: hypertonic), adjusted by the addition of NaCl solutions at different concentrations in pre-transfection, post-transfection, and/or pre- and post-transfection.

promote the sedimentation of nanoparticles onto the cells[40]. This finding is important because it not only substantially increases the transfection efficiency but also has the potential to reduce the cost of the transfection procedure. A similar increase in transfection efficiency for lymphocyte cells using 24-armed poly(2-dimethylamino) ethyl methacrylate (PDMAEMA) in tubes compared to plates has been reported by another research group[22].

### 3.12. Transfection settings: direct and revers

Today, various approaches have been employed to induce the movement of nanoparticles toward cells. Techniques such as electroporation and magnetic transfection actively facilitate the transport of nanoparticles to the cell surface. In contrast, passive transfection using polymers primarily relies on the Brownian motion of nanoparticles and their sedimentation onto the cell surface due to gravitational forces. Consequently, we evaluated the effects of nanoparticles movements toward the cells and vice versa through direct and reverse transfections, respectively. As shown in Fig. 5a direct transfection, where nanoparticles are moved toward the cells, resulted in two-fold higher luciferase activity in the plate setting, suggesting improved transfection efficiency. Conversely, reverse transfection exhibited ten-fold higher luciferase activity in the vial setting. This discrepancy may be attributed to the different dynamics of nanoparticle-cell interactions in each setup. In the plate setting, direct contact between nanoparticles and cells likely facilitates more efficient uptake. In contrast, the vial setting may allow for better mixing and interaction between nanoparticles and cells, thereby enhancing reverse transfection efficiency. Our results are consistent with those reported by Riedl et al., who found that reverse transfection of Jurkat cells using PDMAEMA polymer led to improved transfection efficiency[22].

### 3.13. The effect of acidity of extracellular media on transfection

One of the primary factors that determines the intracellular fate of gene delivery nanocarriers is their ability to escape from endosomes. In the case of PEI, the protonation of amine groups is a key mechanism facilitating endosomal escape, which is significantly influenced by endosomal acidification. Therefore, we investigated the effect of extracellular pH on the transfection efficiency of PEI/DNA nanoparticles in T cells. As shown in Fig. 5b, the transfection rate of the nanoparticles correlated with the extracellular acidity of the medium. Specifically, an increase in extracellular pH from 7.0 to 9.0 resulted in a 5- to 10-fold increase in luciferase activity in transfected cells, depending on the N/ P ratios. Interestingly, we observed a higher transfection rate at medium with a pH value of 5.0 compared to 6.0. These results suggest that an increase in extracellular pH and hydroxide ion concentration may trigger enhanced hydrogen ion production within cells. This response likely serves as a defense mechanism against elevated extracellular alkalinity. Notably, the increased acidification of endosomes amplifies the 'proton sponge' effect associated with polyethylenimine (PEI). This effect disrupts the endosomal membrane, facilitating the escape of genetic material carried by PEI from the endosome into the cytoplasm, thereby enhancing transfection efficiency. Furthermore, the endosomes of T cells show a lower acidification rate compared to other nonadherent cells. This phenomenon reduces the efficiency of transfection agents that rely on a pH-triggered endosomal escape mechanism. Overall, this low transfection efficiency necessitates efforts to improve transfection methods [4,12,13,32]. The Pun group reported that one of the main factors differentiating the transfection efficiency of adherent and non-adherent cells is the lower endosomal and intracellular acidity levels in T cells[32]. This finding suggests that employing alternative endosomal escape mechanisms and increasing endosomal acidity may enhance the efficiency of gene delivery to T cells.

3.14. The effect of tonicity of extracellular media on transfection efficiency

The cell membrane is the primary barrier against the uptake of nanoparticles. The integrity of the cell membrane can be influenced by the tonicity of the extracellular medium. Therefore, we evaluated the effect of medium tonicity on the efficiency of PEI/DNA complexes for the transfection of T cells. As shown in Figs. 5c and 5d, hypotonic medium enhanced the efficiency of PEI-mediated gene delivery to cells compared to hypertonic medium. Furthermore, adjusting the medium to hypotonic (NaCl 0.5 % w/v) after the addition of the complexes resulted in a higher transfection rate than adjusting the medium to hypotonic just before the addition of the complexes. Notably, adjusting the medium to hypotonic both pre- and post-transfection resulted in the highest transfection rate among other conditions tested. These findings suggest that hypotonic media, particularly at a NaCl concentration of 0.5 % w/v, facilitate the uptake of PEI/DNA nanoparticles. Previous studies have indicated that T cells exhibit a reduced rate of endocytosis, although the reasons for this low endocytosis efficiency remain unclear. Research suggests that PEI primarily interacts with negatively charged membrane proteins, such as sulfated proteoglycans, to mediate cellular internalization[22]. Interestingly, our results demonstrate that the use of hypotonic medium significantly enhances the transfection rate of T cells.

### 3.15. Cytotoxicity studies

One of the key factors influencing the transfection efficiency of nanoparticles is the toxicity associated with both the nanoparticles themselves and their nanocarrier counterparts. Consequently, researchers are focused on mitigating this undesirable effect. In our study, we evaluated the safety levels of nanocarriers and nanoparticles under various conditions for the transfection of Jurkat cells. As shown in Fig. 6a, the free carriers at high concentrations reduced the viability of Jurkat cells, presumably due to their high positive charges, which resulted in increased toxicity. Interestingly, a similar outcome was observed with the PEI-cholesterol conjugate [41]. However, complexation with DNA diminished the carrier-associated toxicity (Fig. 6b). At a concentration of  $4 \mu g/100 \mu l$  of medium of the carriers, cell viability decreased to approximately 50 %. In contrast, in the presence of DNA, cell viability was around 80 % at N/P ratios below 10. Nevertheless, at N/P ratios exceeding 10, we observed significant toxicity. These results suggest that DNA neutralizes the high positive charge of the nanocarriers, thereby preventing a decline in cell viability. However, at high N/P ratios, the complex solution contains a larger fraction of free carriers that exist without actively participating in the nanoparticle structure, thereby inducing toxicity. The optimal transfection rate was achieved at N/P ratios lower than 10. The clear advantage of utilizing nanoparticles with the optimal N/P ratio is a higher transfection rate coupled with a more favorable safety profile compared to using very low or very high N/P ratios. We also evaluated the effect of varying medium acidity on the viability of T-cells in the presence and absence of PEI/DNA nanoparticles. As shown in Fig. 6b, both a decrease and an increase in extracellular pH reduced cell viability. The lowest viability was observed at an extracellular pH of 5.5 in the presence of nanoparticles, which decreased viability to approximately 50 %. However, as shown in Figs. 6c and 6d, PEI/DNA nanoparticles exhibited maximum transfection rates and very low cytotoxic effects in T cells at an extracellular pH of 9.0 [42].

### 3.16. Evaluation of the uptake of PEI/DNA Nanoparticles

T cells are often noted for their lower endocytosis rate compared to other cell types. In this study, we evaluated the effects of various parameters on the uptake rate of PEI/DNA nanoparticles. As illustrated in Fig. 7a and b, control cells transfected in the plate exhibited a low rate of cellular uptake of nanoparticles. Conversely, the use of hypotonic

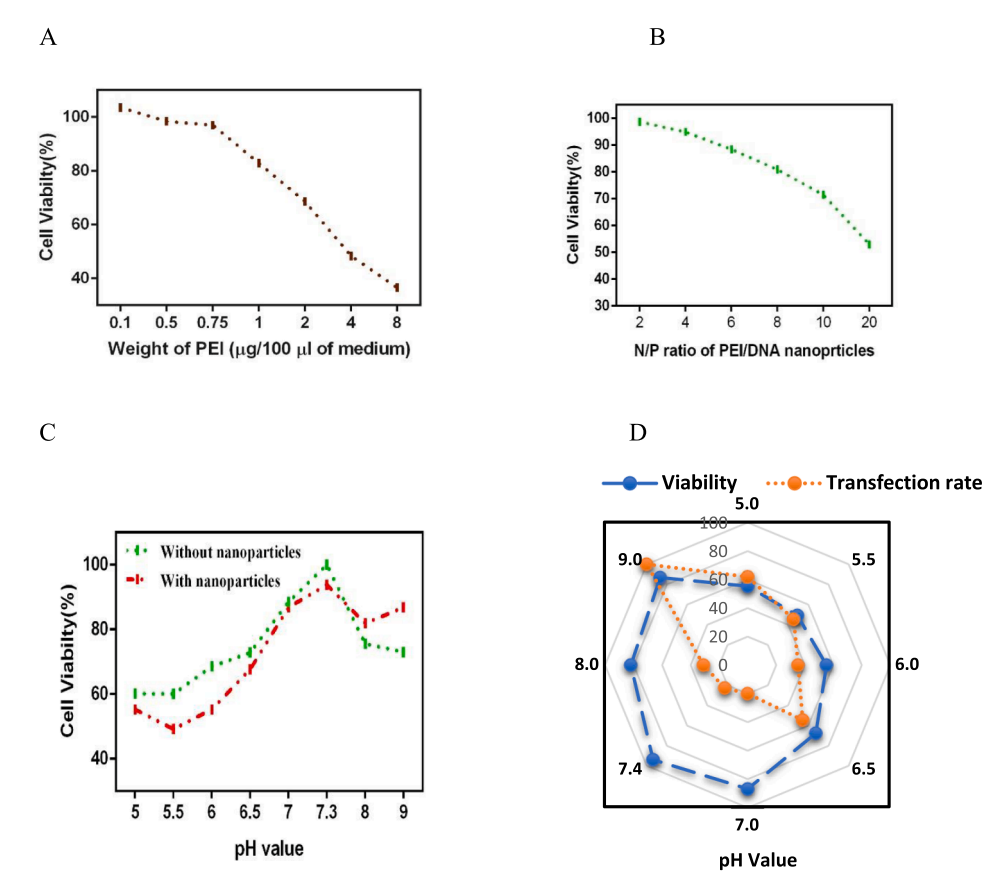


Fig. 6. Cytotoxicity profiles and evaluation of the effect of acidity on cytotoxicity and transfection. A) Evaluation of cytotoxicity of various amounts of free PEI on T cells. B) Evaluation of cytotoxicity of nanoparticles of PEI/DNA on T cells. C) Analysis of the effect of transfection media acidity on T cell viability in the presence and absence of nanoparticles of PEI/DNA complexes. D) Optimization of the acidity of transfection medium to identify the optimal conditions for transfection while ensuring a favorable safety profile.

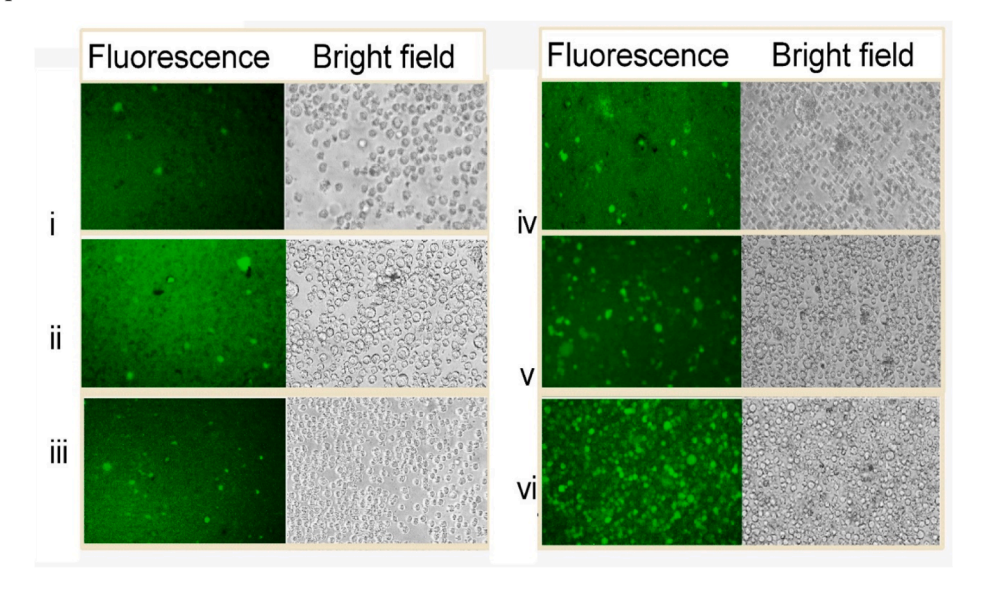
medium increased the uptake rate by approximately two-fold compared to the control (Fig. 7a-i). This result aligns with the findings from the luciferase gene transfection assay. Furthermore, altering the acidity of the medium to pH 5 and pH 9 did not significantly affect the cellular uptake rate. This observation confirms that changes in pH, by affecting endosomal conditions, can enhance the transfection rate. As shown in Fig. 7a-iv, reverse transfection of cells in vials resulted in more than a 20-fold increase in fluorescent cells compared to the control. This observation suggests that modifying the transfection method increased the possibility of interaction between cells and nanoparticles, while also exploiting gravitational forces to enhance uptake and, in turn, gene delivery rates. Surprisingly, when combining reverse transfection in vials with hypotonic medium, we observed a 40-fold increase in the number of bright fluorescent cells compared to the control (Fig. 7b). This finding indicates a synergistic effect between hypotonic medium and reverse transfection. In a related study, Liu et al. developed an acoustothermal transfection method that improves membrane and nuclear envelope permeability, enabling high-throughput delivery of plasmids into primary T cells with high efficiency [43].

## 3.17. Evaluation of the effects of temperature and buffer on nanoparticle stability during storage

One of the primary parameters for an effective transfection agent is its potential for long-term storage. To evaluate this aspect, we investigated the effects of buffer and temperature on the stability of DNA binding capacity and the size of nanoparticles. As illustrated in Fig. 8a, nanoparticles suspended in deionized water at 25  $^{\circ}$ C a minimum size around 200 nm. However, beyond this point, the nanoparticles began to interact more, leading to aggregation and an increase in size to

600-800 nm after 24 hours, which may be attributed to this aggregation. González-Domínguez et al. reported a comparable trend in the aggregation of PEI/DNA complexes[21]. After 3 days, the size of the nanoparticles reduced to 600 nm, presumably due to the release of DNA. Furthermore, after 5 days, the size fluctuated again to 2000 nm, which may be attributed to particle de-condensation. This observation is consistent with the findings from the release study, which supports the notion of particle de-condensation. Although nanoparticles diluted in water and stored at 4 °C and -20 °C showed a similar trend, those stored at -20 °C exhibited a larger size at various time points compared to those stored at 25 °C and 4 °C. This discrepancy is presumably due to the effects of the freeze-thaw process on particle integrity. In the investigation of nanoparticles suspended in phosphate-buffered saline (PBS) at 25 °C, dynamic light scattering (DLS) results revealed an initial size of approximately 280 nm and after one day, the size increased to 2 µm suggesting a propensity for aggregation in an ionic environment (Fig. 8b). The presence of salts in PBS may enhance inter-particles interactions, leading to clustering and an increased hydrodynamic radius [44]. In contrast, nanoparticles stored in PBS at 4 °C exhibited minimal size fluctuations and a lower rate of size increase compared to those maintained at higher temperatures, implying that lower temperatures contribute to the stabilization of PEI/DNA complexes by reducing kinetic energy and inhibiting aggregation. However, nanoparticles stored at -20 °C in PBS demonstrated a significant increase in size, reaching approximately 2 µm after 5 days, indicating that the ionic environment exacerbates the effects of freeze-thaw cycles on particles size and decondensation. Furthermore, nanoparticles stored in RPMI media at 25 °C maintained a stable size for 3 days, averaging around 300 nm, which suggests that the nutrient-rich components in RPMI 1640 may play a stabilizing role under moderate conditions (Fig. 8c). Conversely,

Α



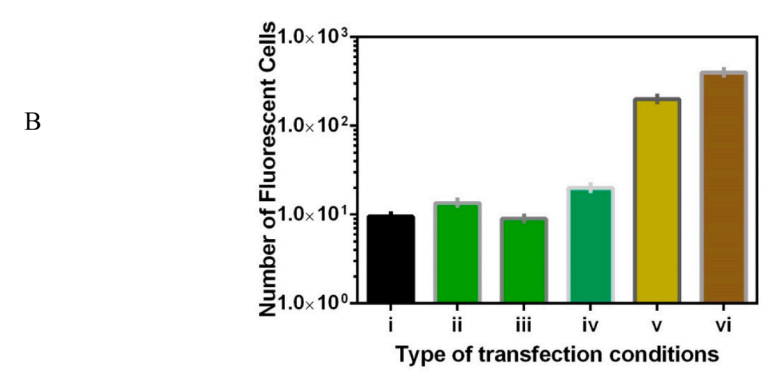


Fig. 7. Evaluation of the effect of various transfection conditions on cellular uptake of PEI/DNA nanoparticles A) Fluorescence microscopy images of Jurkat cells transfected with PEI in complex with fluorescent DNA at an N/P ratio of 8 under different conditions, including: i) Direct transfection in a plate with RPMI 1640 media at pH 7.4 (control). ii) Direct transfection in a plate with RPMI 1640 media at pH 5.0. iii) Direct transfection in a plate with RPMI 1640 media at pH 9.0. iv) Direct transfection in a plate with hypotonic media. v) Reverse transfection in a vial with RPMI 1640 media. Vi) Reverse transfection in a vial with RPMI 1640 media. B) Quantification of the uptake rate of PEI/DNA nanoparticles into Jurkat cells under different transfection conditions.

nanoparticles stored at -20 °C exhibited a substantial increase in size on the first day of storage, highlighting the high sensitivity of PEI/DNA particles to freeze-thaw processes. Notably, nanoparticles stored in RPMI 1640 at 4 °C showed a larger size compared to those at 25 °C; yet particle size remained relatively consistent at lower temperatures over a period of 5 days. Overall, in all conditions, the gradual increase in average size suggests that particle de-condensation is a continuous process in ionic and nutrient-rich media, further exacerbated by freeze-thaw conditions. PEI/DNA complexes demonstrated greater stability in nutrient-rich RPMI 1640 medium, particularly during days 1–3, indicating partial stability that is dependent on the thermal environment. In contrast, PEI/DNA complexes in ionic buffers like PBS tend to aggregate more rapidly, resulting in increased particle sizes over time, especially under elevated temperatures. Surprisingly, PBS at 4 °C was the most suitable condition for long-term storage of PEI/DNA particles, minimizing size variations and aggregation while ensuring particle stability over time.

Moreover, as shown in Fig. 8d, nanoparticles retained their DNA binding capacity across all temperatures and buffer conditions throughout the 7-day stability test. These findings highlight the importance of selecting appropriate buffer and temperature conditions for the storage and manipulation of PEI/DNA complexes. Future studies may focus on optimizing buffer formulations or incorporating stabilizing

agents to enhance the robustness of PEI/DNA nanoparticles under various conditions.

### 3.18. Limitations and benefits

This optimization study, opens new avenues for the design of lowcost and high-efficiency non-viral gene delivery systems, thereby enabling the production of engineered T cells for clinical purposes. Moreover, this optimized transfection process can be extensively and easily utilized in screening experiments for the tailoring and manufacturing of CAR T cells. The design of novel and efficient CAR T cells necessitates iterative engineering of the CAR structure; thus, using this optimized PEI/DNA nanoparticle-based gene delivery provides a rapid tool for the screening and selection of CAR constructs without the need to provide new viral carriers for each construct[16]. More importantly, one of the main approaches to reducing the cost of CAR T cells is the use of inexpensive non-viral gene delivery methods instead of traditional viral gene delivery methods. In other words, this study demonstrates a cost-effective and efficient approach to non-viral gene delivery to T cells, which is pivotal for clinical applications. The optimized complexation process facilitates broader use in screening experiments, accelerating the development of CAR T cells. In terms of limitations, the scope of this study may be restricted to certain T cells

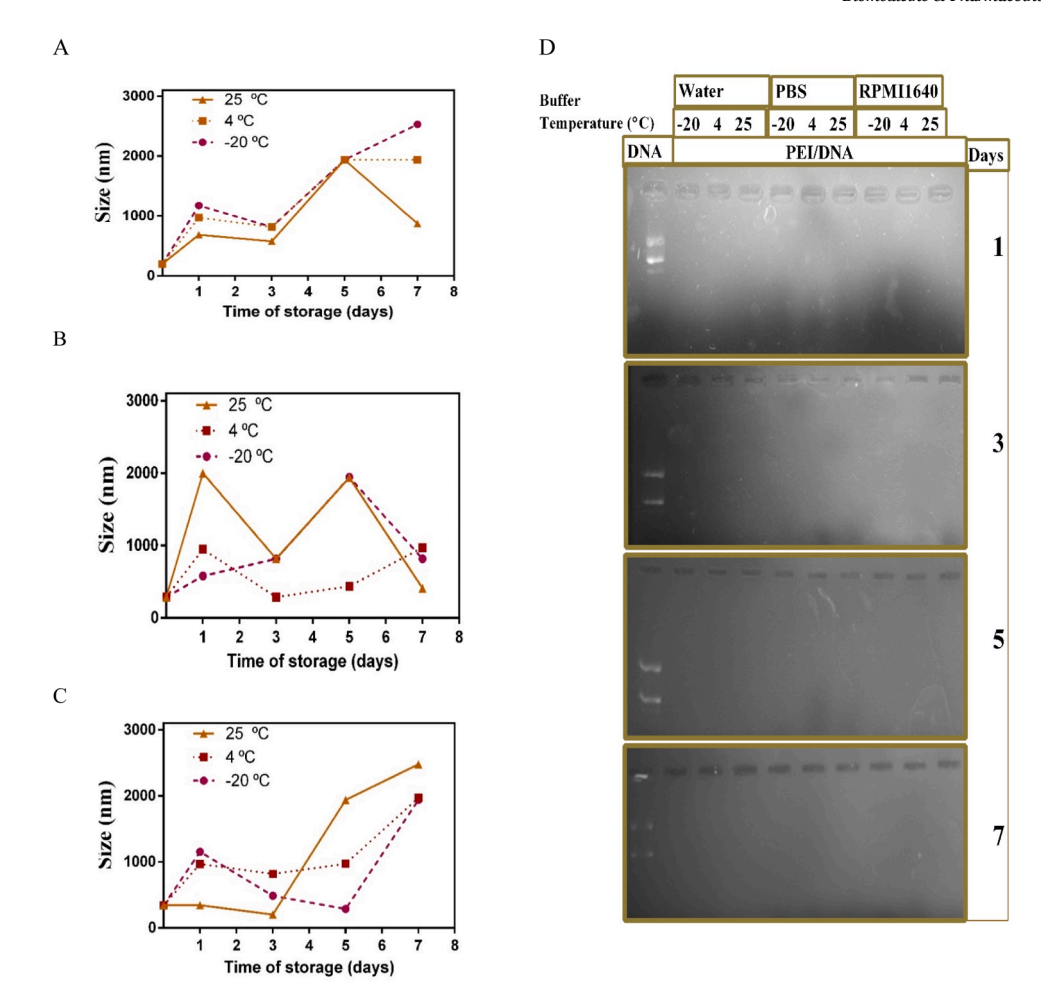


Fig. 8. Evaluation of the storage stability of PEI/DNA nanoparticles. PEI/DNA nanoparticles were prepared at an N/P ratio of 8 using 1  $\mu$ g of DNA. The nanoparticles were diluted with deionized water (A), phosphate-buffered saline (B), and RPMI 1640 (C) and then stored for several days at various temperatures. The size of the nanoparticles was analyzed using dynamic light scattering (DLS), (D). Gel retardation assay was conducted to evaluate the DNA binding capability of the stored nanoparticles.

populations, and its applicability to other cell types remains to be explored. Moreover, while high PEI binding capacity is advantageous for initial complex formation, it may inadvertently hinder subsequent DNA release, negatively impacting transfection efficiency. This observation underscores the delicate balance between binding capacity and release efficiency in optimizing transfection protocols. Additionally, the long-term efficacy of the optimized nanoparticles in various therapeutic contexts have yet to be established, necessitating further investigation.

### 4. Conclusions

Immune cell engineering has recently gained significant attention due to its potential clinical applications. Various strategies have been devised to assist in the genetic manipulation of T cells, which play a crucial role in immunotherapy. The development and enhancement of gene delivery methods are critical, given the hard-to-transfect nature of these cells. In this study, we aimed to comprehensive evaluation of the factors influencing PEI-mediated transfection of T cells. The PEI was complexed with DNA to form size- and charge-tunable nanoparticles that remained stable in the presence of serum nucleases. The release study validated that, the nanoparticles at an N/P ratio of 2 released a greater amount of DNA compared to those at an N/P ratio of 8. Using a luciferase gene reporter, we found that PEI/DNA nanoparticles effectively transfected Jurkat cells at an N/P ratio of 8, which differed from the observations made in adherent cells. More importantly, the nanoparticles at this N/P ratio demonstrated an acceptable safety profile in

Jurkat cells. Furthermore, we determined that 2000 cells per µl of medium and a dose of  $2\,\mu g$  per  $100\,\mu L$  of medium yielded the highest transfection efficiency. Notably, our results indicated that transfection in a 1.5 ml vial instead of a tissue culture plate, resulted in a higher transfection rate in Jurkat cells. This is presumably due to the reduced space, which increases the probability of interaction between cells and nanoparticles. Surprisingly, the results of this study confirmed that transfection in a vial versus a plate exhibited different efficiencies in reverse and direct approaches. Moreover, modulating cellular physiology by adjusting the acidity and tonicity of the transfection medium significantly enhanced PEI-mediated transfection of T cells. Additionally, the cellular uptake study confirmed that reverse transfection in a vial and the use of hypotonic medium intensified the uptake of nanoparticles. Importantly, the nanoparticles remained relatively stable in RPMI 1640 medium at 25°C with an appropriate size for 3 days, and in PBS at 4°C for 7 days. We believe that the findings of our experiment may be applicable in high-cost studies aimed at developing novel immune-engineered T cells.

### **Funding**

This work was financially supported by Jahrom University of Medical Sciences (Grant ID: 402000097).

### CRediT authorship contribution statement

Hassan Bardania: Supervision, Methodology, Investigation. Fatemeh Askari: Methodology, Conceptualization. Jalil Mehrzad: Resources, Investigation, Conceptualization. Saman Hosseinkhani: Resources, Funding acquisition, Formal analysis, Conceptualization. mohsen alipour: Writing – review & editing, Writing – original draft, Supervision, Software, Resources, Project administration, Methodology, Investigation, Funding acquisition, Formal analysis, Data curation. Abazar Roustazadeh: Resources, Project administration, Methodology, Investigation, Funding acquisition, Formal analysis, Conceptualization. Maryam Askari: Visualization, Validation, Software, Methodology, Formal analysis. Mohammad Hossein Heidari: Methodology. Majid Kowsari: Methodology, Conceptualization.

### **Declaration of Competing Interest**

The authors declare that they have no known competing financial interests or personal relationships that could have appeared to influence the work reported in this paper.

### Acknowledgements

This study was also approved by the Ethics Committee of Jahrom University of Medical Sciences (Approval ID: IR.JUMS.REC.1402.142). We express our gratitude to Mohammad Aref Bagherzadeh, Ali Torabi, and Ramin Jamali for their invaluable assistance in the processes of plasmid preparation, gel retardation, and serum stability testing.

### Data availability

Data will be made available on request.

### References

- [1] Y. Xie, N.H. Kim, V. Nadithe, D. Schalk, A. Thakur, A. Kılıç, L.G. Lum, D.J. Bassett, O.M. Merkel, Targeted delivery of siRNA to activated T cells via transferrinpolyethylenimine (Tf-PEI) as a potential therapy of asthma, J. Control. Release 229 (2016) 120-129
- [2] K. Paris, L.A. Wall, The treatment of primary immune deficiencies: lessons learned and future opportunities, Clin. Rev. Allergy Immunol. 65 (1) (2023) 19–30.
- [3] H. Moffett, M. Coon, S. Radtke, S. Stephan, L. McKnight, A. Lambert, B. Stoddard, H. Kiem, M. Stephan, Hit-and-run programming of therapeutic cytoreagents using mRNA nanocarriers, Nat. Commun. 8 (1) (2017) 389.
- [4] E. Harris, D. Zimmerman, E. Warga, A. Bamezai, J. Elmer, Nonviral gene delivery to T cells with Lipofectamine LTX, Biotechnol. Bioeng. 118 (4) (2021) 1674–1687.
- [5] P.S. Kozani, M.A. Shokrgozar, M. Evazalipour, M.H. Roudkenar, CRISPR/Cas9-medaited knockout of endogenous T-cell receptor in Jurkat cells and generation of NY-ESO-1-specific T cells: an in vitro study, Int. Immunopharmacol. 110 (2022) 120055
- [6] Y. Qu, Z.S. Dunn, X. Chen, M. MacMullan, G. Cinay, H.-y Wang, J. Liu, F. Hu, P. Wang, Adenosine deaminase 1 overexpression enhances the antitumor efficacy of chimeric antigen receptor-engineered T cells, Hum. Gene Ther. 33 (5-6) (2022) 223–236.
- [7] A. Kremer, T. Ryaykenen, R. Haraszti, Systematic optimization of siRNA productive uptake into resting and activated T cells ex vivo, Biomed. Pharmacother. 172 (2024) 116285.
- [8] V. Perri, M. Pellegrino, F. Ceccacci, A. Scipioni, S. Petrini, E. Gianchecchi, A. Lo Russo, S. De Santis, G. Mancini, A. Fierabracci, Use of short interfering RNA delivered by cationic liposomes to enable efficient down-regulation of PTPN22 gene in human T lymphocytes, PLoS One 12 (4) (2017) e0175784.
- [9] A. Kheirolomoom, A.J. Kare, E.S. Ingham, R. Paulmurugan, E.R. Robinson, M. Baikoghli, M. Inayathullah, J.W. Seo, J. Wang, B.Z. Fite, In situ T-cell transfection by anti-CD3-conjugated lipid nanoparticles leads to T-cell activation, migration, and phenotypic shift, Biomaterials 281 (2022) 121339.
- [10] X. Liang, J. Potter, S. Kumar, Y. Zou, R. Quintanilla, M. Sridharan, J. Carte, W. Chen, N. Roark, S. Ranganathan, Rapid and highly efficient mammalian cell engineering via Cas9 protein transfection, J. Biotechnol. 208 (2015) 44–53.
- [11] G.M. Redpath, M. Ecker, N. Kapoor-Kaushik, H. Vartoukian, M. Carnell, D. Kempe, M. Biro, N. Ariotti, J. Rossy, Flotillins promote T cell receptor sorting through a fast Rab5–Rab11 endocytic recycling axis, Nat. Commun. 10 (1) (2019) 4392.
- [12] I. Rahimmanesh, M. Totonchi, H. Khanahmad, The challenging nature of primary T lymphocytes for transfection: effect of protamine sulfate on the transfection efficiency of chemical transfection reagents, Res. Pharm. Sci. 15 (5) (2020) 437.

- [13] C.J. McKinlay, N.L. Benner, O.A. Haabeth, R.M. Waymouth, P.A Wender, Enhanced mRNA delivery into lymphocytes enabled by lipid-varied libraries of chargealtering releasable transporters, Proc Natl Acad Sci 115 (26) (2018) E5859–E5866.
- [14] R. Xiong, D. Hua, J. Van Hoeck, D. Berdecka, L. Léger, S. De Munter, J.C. Fraire, L. Raes, A. Harizaj, F. Sauvage, Photothermal nanofibres enable safe engineering of therapeutic cells, Nat. Nanotechnol. 16 (11) (2021) 1281–1291.
- [15] T. Bo, C. Wang, D. Yao, Q. Jiang, Y. Zhao, F. Wang, W. He, W. Xu, H. Zhou, M. Li, Efficient gene delivery by multifunctional star poly (β-amino ester) s into difficultto-transfect macrophages for M1 polarization, J. Control. Release 368 (2024) 157–169.
- [16] B.R. Olden, Y. Cheng, L.Y. Jonathan, S.H. Pun, Cationic polymers for non-viral gene delivery to human T cells, J. Control. Release 282 (2018) 140–147.
- [17] A. Ahmad, J.M. Khan, B.A. Paray, K. Rashid, A. Parvez, Endolysosomal trapping of therapeutics and endosomal escape strategies, Drug Discov. Today (2024) 104070.
- [18] J. Casper, S.H. Schenk, E. Parhizkar, P. Detampel, A. Dehshahri, J. Huwyler, Polyethylenimine (PEI) in gene therapy: current status and clinical applications, J. Control. Release 362 (2023) 667–691.
- [19] A.P. Rajendran, O. Ogundana, L.C. Morales, D.N. Meenakshi Sundaram, C. Kucharski, R. Kc, H. Uludağ, Transfection efficacy and cellular uptake of lipid-modified polyethyleneimine derivatives for anionic nanoparticles as gene delivery vectors, ACS Appl. Bio Mater. 6 (3) (2023) 1105–1121.
- [20] V.A. Ayyadevara, K.-H. Roh, Calcium enhances polyplex-mediated transfection efficiency of plasmid DNA in Jurkat cells, Drug Deliv. 27 (1) (2020) 805–815.
- [21] I. González-Domínguez, N. Grimaldi, L. Cervera, N. Ventosa, F. Gòdia, Impact of physicochemical properties of DNA/PEI complexes on transient transfection of mammalian cells, N. Biotechnol. 49 (2019) 88–97.
- [22] S.A. Riedl, P. Kaiser, A. Raup, C.V. Synatschke, V. Jérôme, R. Freitag, Non-viral transfection of human T lymphocytes, Processes 6 (10) (2018) 188.
- [23] R. Cheraghi, M. Alipour, M. Nazari, S. Hosseinkhani, Optimization of conditions for gene delivery system based on PEI, Nanomed. J. 4 (1) (2017) 8–16.
- [24] V.A. Ayyadevara, K.H. Roh, Calcium enhances polyplex-mediated transfection efficiency of plasmid DNA in Jurkat cells, Drug Deliv. 27 (1) (2020) 805–815.
- [25] A. Raup, U. Stahlschmidt, V. Jérôme, C.V. Synatschke, A.H. Müller, R.J.P. Freitag, Influence of polyplex formation on the performance of star-shaped polycationic transfection agents for mammalian cells 8 (6) (2016) 224.
- [26] M. Alipour, S. Hosseinkhani, R. Sheikhnejad, R. Cheraghi, Nano-biomimetic carriers are implicated in mechanistic evaluation of intracellular gene delivery, Sci. Rep. 7 (2017).
- [27] R. Cheraghi, M. Nazari, M. Alipour, A. Majidi, S. Hosseinkhani, Development of a targeted anti-HER2 scFv chimeric peptide for gene delivery into HER2-positive breast cancer cells, Int. J. Pharm. 515 (1-2) (2016) 632–643.
- [28] M. Alipour, A. Majidi, F. Molaabasi, R. Sheikhnejad, S. Hosseinkhani, In vivo tumor gene delivery using novel peptideticles: pH-responsive and ligand targeted core-shell nanoassembly, Int. J. Cancer 143 (8) (2018) 2017–2028.
- [29] A. Raup, U. Stahlschmidt, V. Jérôme, C.V. Synatschke, A.H. Müller, R. Freitag, Influence of polyplex formation on the performance of star-shaped polycationic transfection agents for mammalian cells, Polymers 8 (6) (2016) 224.
- [30] S.K. Filippov, R. Khusnutdinov, A. Murmiliuk, W. Inam, L.Y. Zakharova, H. Zhang, V.V. Khutoryanskiy, Dynamic light scattering and transmission electron microscopy in drug delivery: a roadmap for correct characterization of nanoparticles and interpretation of results, Mater. Horiz. 10 (12) (2023) 5354–5370.
- [31] A. Amani, T. Kabiri, S. Shafiee, A. Hamidi, Preparation and characterization of PLA-PEG-PLA/PEI/DNA nanoparticles for improvement of transfection efficiency and controlled release of DNA in gene delivery systems, Iran. J. Pharm. Res.: IJPR 18 (1) (2019) 125.
- [32] B.R. Olden, E. Cheng, Y. Cheng, S.H. Pun, Identifying key barriers in cationic polymer gene delivery to human T cells, Biomater. Sci. 7 (3) (2019) 789–797.
- [33] A.M. Ansari, A.K. Ahmed, A.E. Matsangos, F. Lay, L.J. Born, G. Marti, J. W. Harmon, Z. Sun, Cellular GFP toxicity and immunogenicity: potential confounders in in vivo cell tracking experiments, Stem Cell Rev. Rep. 12 (2016) 553–559.
- [34] S.-X. Xie, A.A. Baoum, N.A. Alhakamy, C.J. Berkland, Calcium enhances gene expression when using low molecular weight poly-L-lysine delivery vehicles, Int. J. Pharm. 547 (1-2) (2018) 274–281.
- [35] T. Jiang, C. Zhou, S. Ren, Role of IL-2 in cancer immunotherapy, Oncoimmunology 5 (6) (2016) e1163462.
- [36] J. Wagner, V. Pfannenstiel, A. Waldmann, J.W. Bergs, B. Brill, S. Huenecke, T. Klingebiel, F. Rödel, C.J. Buchholz, W.S. Wels, A two-phase expansion protocol combining interleukin (IL)-15 and IL-21 improves natural killer cell proliferation and cytotoxicity against rhabdomyosarcoma, Front. Immunol. 8 (2017) 676.
- [37] L. Xie, J. Wang, L. Song, T. Jiang, F. Yan, Cell-cycle dependent nuclear gene delivery enhances the effects of E-cadherin against tumor invasion and metastasis, Signal Transduct. Target. Ther. 8 (1) (2023) 182.
- [38] S. Mancinelli, A. Turcato, A. Kisslinger, A. Bongiovanni, V. Zazzu, A. Lanati, G. L. Liguori, Design of transfections: implementation of design of experiments for cell transfection fine tuning, Biotechnol. Bioeng. 118 (11) (2021) 4488–4502.
- [39] D.O. Forcato, A. Fili, F.E. Alustiza, J.M. Lazaro Martinez, S. Bongiovanni Abel, M. F. Olmos Nicotra, A.P. Alessio, N. Rodríguez, C. Barbero, P. Bosch, Transfection of bovine fetal fibroblast with polyethylenimine (PEI) nanoparticles: effect of particle size and presence of fetal bovine serum on transgene delivery and cytotoxicity, Cytotechnology 69 (2017) 655–665.
- [40] Y. Chen, S. Aslanoglou, G. Gervinskas, H. Abdelmaksoud, N.H. Voelcker, R. Elnathan, Cellular deformations induced by conical silicon nanowire arrays facilitate gene delivery, Small 15 (47) (2019) 1904819.

- [41] M. Monajati, S. Tavakoli, S.S. Abolmaali, G. Yousefi, A. Tamaddon, Effect of PEGylation on assembly morphology and cellular uptake of poly ethyleneiminecholesterol conjugates for delivery of sorafenib tosylate in hepatocellular carcinoma. BioImpacts: B1 8 (4) (2018) 241.
- carcinoma, BioImpacts: BI 8 (4) (2018) 241.

  [42] S. Lee, A. Shanti, Effect of exogenous pH on cell growth of breast cancer cells, Int. J. Mol. Sci. 22 (18) (2021) 9910.
- [43] X. Liu, N. Rong, Z. Tian, J. Rich, L. Niu, P. Li, L. Huang, Y. Dong, W. Zhou, P. Zhang, Acoustothermal transfection for cell therapy, Sci. Adv. 10 (16) (2024) eadk1855.
- [44] I. González-Domínguez, E. Puente-Massaguer, J. Lavado-García, L. Cervera, F. Gòdia, Micrometric DNA/PEI polyplexes correlate with higher transient gene expression yields in HEK 293 cells, N. Biotechnol. 68 (2022) 87–96.